ChemComm

COMMUNICATION

View Article Online
View Journal | View Issue

Cite this: *Chem. Commun.*, 2019, **55**, 14653

Received 5th September 2019,
Accepted 12th November 2019

DOI: 10.1039/c9cc06942a

rsc.li/chemcomm

Multitasking polyamine/ferrioxalate nano-sized assemblies: thermo-, photo-, and redox-responsive soft materials made easy†

Santiago E. Herrera,‡[a] Maximiliano L. Agazzi,‡[a] M. Lorena Cortez,[a] Waldemar A. Marmisollé,[a] Mario Tagliazucchi*[b] and Omar Azzaroni*[a]

Responsive nanomaterials have emerged as key components in materials sciences. Herein, we report the one-step preparation of multi-stimuli responsive polyamine-salt aggregates (PSA) by ionically crosslinking polyethylenimine with potassium ferrioxalate (FeOx). The unique properties of FeOx enables a novel class of soft nanomaterial that disassembles by exposure to light, reducing environments and temperature.

Nanoparticles capable of changing their properties in response to stimuli have been widely explored for multiple applications.[1–3] Depending on the chemical properties of the nanoparticle, a stimulus can trigger aggregation (instructed-assembly),[4] shape transformation or complete dissolution.[5–7] Multi-stimuli responsive nanoparticles are able to respond to more than one type of stimuli, which makes them very attractive materials in biotechnology and nanotechnology.[8–10] Different multi-stimuli responsive systems have been developed such as polymers, microgels, micelles, vesicles, dendrimers, liquid crystals and films.[11–14] A common design strategy for the synthesis of multi-stimuli responsive materials involves combining in a single material different chemical motifs that confer responsiveness to different stimuli.[15,16] Such strategy demands multi-step synthetic routes that increase costs and hinder the scalability necessary for technological applications.

Polyamine-salt aggregates (PSAs), constituted of ionically crosslinked polyelectrolyte networks, have gained interest due to their straightforward synthesis, nanometre-size, capacity to load functional compounds, integration in surface films, and stimuli-triggered disassembly.[17–19] As the electrostatic interaction between the polycation and the anionic crosslinker represents the major contribution to the stability of PSAs,[20,21] the regulation of charges is a key factor in order to drive the system either to self-assemble or disassemble.[22]

In order to rationally create a multi-stimuli responsive PSA, the crosslinker and/or the polyamine should present defined structural changes with different stimuli. Herein, we introduce potassium ferrioxalate (FeOx) as an ionic crosslinking agent for the formation of PSAs using branched polyethylenimine (PEI) as polyamine. In solution phase, FeOx exists as a (−3)-charged Fe(III)/oxalate chelate complex ($[Fe(III)(C_2O_4)_3]^{3-}$), which is commonly used as an actinometer that undergoes photochemical decomposition when irradiated with light.[23,24] As FeOx is an Fe(III)-based complex, it can also serve as an oxidizing agent in reductive environments forming a (−2)-charged Fe(II)-based complex (ferrooxalate, $[Fe(II)(C_2O_4)_2]^{2-}$) by releasing one oxalate ligand.[23] Here, we demonstrate that the chemistry of FeOx can be exploited for the rational design and construction of a multi-stimuli responsive PSA.

A colloidal suspension of PEI/FeOx-PSAs was obtained by direct mixing of PEI and FeOx aqueous solutions (parent solutions). These solutions were deoxygenated and their pH was adjusted to 4.5 in order to prevent Fe(II) re-oxidation and precipitation of $Fe(OH)_3$, respectively. Scheme 1 shows the formation of the PEI/FeOx-PSA, which is mainly stabilized by electrostatic interactions between oppositely charged species.[20,21] Upon PEI/FeOx-PSA formation, a net proton uptake from the solution is produced, which raises the pH from 4.5 to 5.8. This pH-shifting effect is attributed to the protonation of initially non-protonated amine groups in PEI, favoured by the condensation of polymer chains with FeOx complexes acting as anionic crosslinkers.[21] A detailed description of the PSA formation process has been previously reported in the literature, showing that the charge of the crosslinker regulates the formation and dissolution of the colloidal dispersion.[21]

After a stabilization period of 24 h, a ζ-potential of +26.7 mV was measured, thus suggesting that PSAs in solution are mainly

[a] *Instituto de Investigaciones Fisicoquímicas Teóricas y Aplicadas (INIFTA) (UNLP, CONICET), Sucursal 4, Casilla de Correo 16, 1900 La Plata, Argentina. E-mail: azzaroni@inifta.unlp.edu.ar; Web: http://softmatter.quimica.unlp.edu.ar, www.twitter.com/softmatterlab*

[b] *Departamento de Química Inorgánica, Analítica y Química Física, INQUIMAE, CONICET. Facultad de Ciencias Exactas y Naturales. Ciudad Universitaria, Pabellón 2, Buenos Aires C1428EHA, Argentina. E-mail: mario@qi.fcen.uba.ar*

† Electronic supplementary information (ESI) available: Experimental procedures, general methods and supporting data (PDF file). Sun-triggered PEI/FeOx-PSA disassembly video, redox-triggered PEI/FeOx-PSA disassembly video, and temperature-triggered PEI/FeOX-PSA disassembly video. See DOI: 10.1039/c9cc06942a

‡ These authors contributed equally.

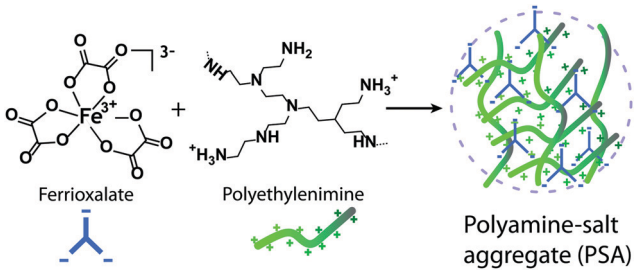

Scheme 1 PEI/FeOx-PSA formation by one-pot/one-step assembly. The supramolecular network of the PSA is mainly stabilized by electrostatic interactions between $-NH_3^+$ groups of PEI and negatively charged FeOx crosslinkers.

stabilized by electrostatic repulsion. Dynamic light scattering (DLS) analysis in Fig. 1b shows a homogeneous distribution of hydrodynamic diameters centred at 210 nm and a polydispersity index of 0.116. Transmission electron microscopy (TEM) analysis depicted in Fig. 1c also shows a sharp distribution of particle sizes with a mean diameter of 180 nm. The TEM image in Fig. 1a shows scorched spheres that are ascribed to PEI/FeOx-PSA particles dehydrated under vacuum. Under ambient conditions, PSAs adsorbed over a flat surface were observed as smooth spheres slightly deformed by surface tension effects (Fig. S1, ESI†).

The internal structure of PSAs was analyzed by IR spectroscopy detecting both PEI and FeOx characteristic bands (Fig. S2, ESI†). We also measured the stoichiometry of the PEI/FeOx-PSA and found a 10 : 1 NH_2 : FeOx molar ratio (see ESI,† file).

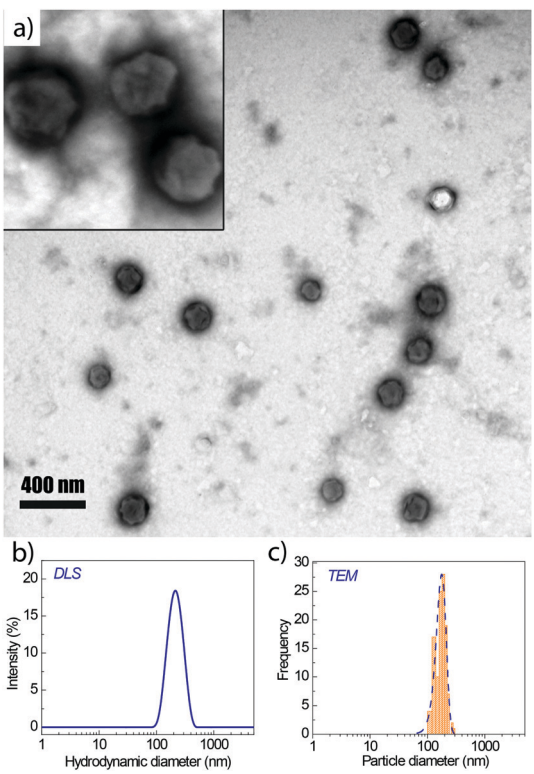

Fig. 1 TEM image of PEI/FeOx-PSAs (a). Inset area: 520 nm × 520 nm. Particle size distributions obtained by DLS (b) and TEM (c).

UV irradiation of the FeOx complex ($[Fe(III)(C_2O_4)_3]^{3-}$) leads to photoinduced electron transfer from the iron center to one of the oxalate ligands.[25] Subsequent chemical processes yield $[Fe(II)(C_2O_4)_2]^{2-}$ and CO_2 as final products with a quantum yield higher than 1,[26,27] see eqn (1).

$$2\left[Fe(III)(C_2O_4)_3\right]^{3-} \xrightarrow{h\nu} 2\left[Fe(II)(C_2O_4)_3\right]^{2-} + C_2O_4^{2-} + 2CO_2 \quad (1)$$

The charge of the crosslinker is crucial to stabilize the structure of PSAs,[20] therefore, we hypothesize that changing it from −3 to −2 (see eqn (1)) may trigger the disassembly of PEI/FeOx-PSAs. To test this idea, a colloidal dispersion of PEI/FeOx-PSAs was directly exposed to sunlight, which resulted in a complete loss of the turbidity in less than 2 min (see ESI,† videos). In order to quantify the light-triggered PEI/FeOx-PSA disassembly, we monitored the process by UV-Vis spectroscopy. For this propose, a PEI/FeOx-PSA sample in a 1 cm quartz cuvette was exposed to UV light in consecutive irradiation periods of 40 s and the full UV-Vis spectrum was recorded after each irradiation step.

Fig. S4 (ESI†) shows the PEI/FeOx-PSA spectra between 350 and 700 nm for increasing irradiation times. The light extinction of the solution decreased with exposure time at all wavelengths, which demonstrates that the colloidal dispersion becomes less dispersive as the sample is irradiated. Knowing that neither PEI nor FeOx absorb light at $\lambda = 580$ nm, the extinction of the solution at that wavelength ($A_{\lambda=580\,nm}$) is completely ascribed to light scattering and, therefore, a decrease in $A_{\lambda=580\,nm}$ can be exclusively attributed to a decrease in the number of PEI/FeOx-PSA particles and/or a reduction in particle size. Fig. 2a shows a linear decrease in $A_{\lambda=580\,nm}$ for the first 4 min of exposure followed by a decrease in the dissolution rate, reaching a value close to zero after 7 min (complete dissolution). In parallel, the particle size was monitored by DLS as shown in Fig. 2b. After an initial lag period of 2 min, the hydrodynamic diameter decreased linearly with exposure time until bad correlogram fitting was detected.

A second strategy to decrease the charge of the crosslinker is the chemical reduction of FeOx as described by eqn (2).

$$\left[Fe(III)(C_2O_4)_3\right]^{3-} \xrightarrow{\text{ascorbic acid}} \left[Fe(II)(C_2O_4)_2\right]^{2-} + C_2O_4^{2-} \quad (2)$$

We added different concentrations of ascorbic acid (AA) to a dispersion of PEI/FeOx-PSA nanoparticles and measured their dissolution kinetics by monitoring the evolution of $A_{\lambda=580\,nm}$ as a function of time. For this, we used a wide range of AA concentrations (0.01 mM–5 mM) in order to cover different FeOx : AA ratios. Fig. 3 shows that in absence of reducing agent the PSA structure remains stable, but AA triggers the dissolution of PEI/FeOx-PSAs with an initial rate that increases with increasing AA concentration. On the other hand, when the AA concentration is high enough, the $A_{\lambda=580\,nm}$ drops to almost zero in less than 5 min, indicating that the PEI/FeOx-PSAs were dissolved (see ESI,† videos).

Interestingly, we observed that the turbidity of the PEI/FeOx-PSA colloidal dispersion was clearly altered by temperature changes in a range close to room temperature. When the temperature of

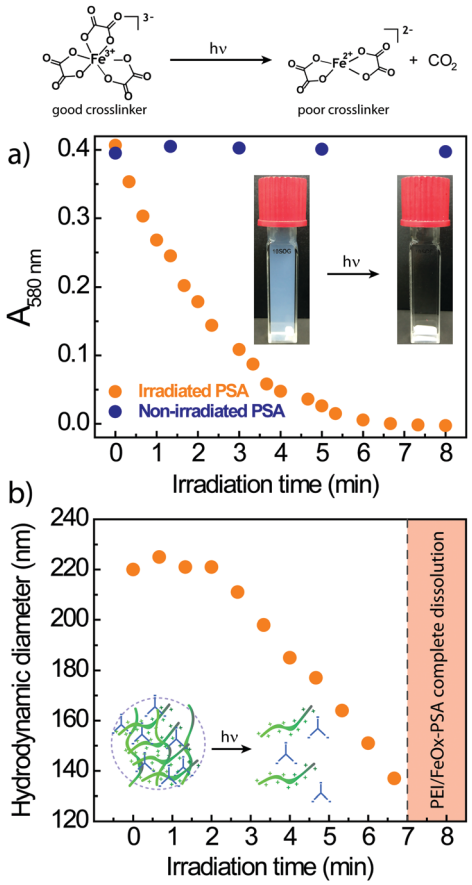

Fig. 2 Light response. Photoinduced dissolution of PEI/FeOx-PSAs. Light extinction at λ = 580 (a) and hydrodynamic diameter (b) as a function of UV irradiation time.

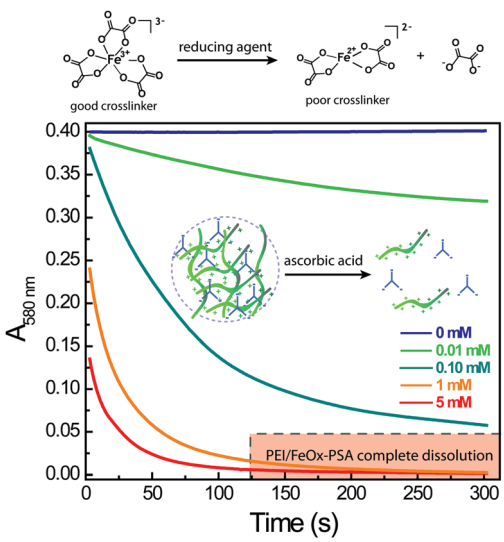

Fig. 3 Redox response. Light extinction at λ = 580 nm as a function of time for a PEI/FeOx-PSA colloidal dispersion immediately after the addition of different concentrations of ascorbic acid (0 mM, 0.01 mM, 0.1 mM, 1 mM and 5 mM).

the PEI/FeOx-PSAs is 5 °C, a cloudy dispersion is observed. However, when the temperature is raised above 35 °C, the solution gets translucent (see ESI,† videos). Notoriously, if the system is cooled down again to 5 °C, the solution gets cloudy as in the first place. This thermal response is unique for the PEI/FeOx system, since we found that similar PSAs like poly(allylamine hydrochloride)/phosphate (PAH/Pi), PAH/tripolyphosphate (PAH/TPP), PEI/TPP and PAH/FeOx do not present appreciable turbidity changes with temperature (data not shown).

In order to understand the nature of the PEI/FeOx-PSA thermal sensitivity, we run a DLS temperature-trend measurement recording both hydrodynamic diameter and derived count rate as a function of temperature from 5 to 55 °C. Fig. 4a shows the variation of the derived count rate with temperature. Fig. S5 (ESI†) shows the evolution of the hydrodynamic diameter in the same conditions. The plots reveal that the size of the PEI/FeOx-PSAs remains almost constant when the temperature increases from 5 to 55 °C, while the derived count rate decays linearly until reaching a constant value of 3000 kcps above 40 °C (negligible PSA concentration). The size of the colloidal complexes is self-limited as a consequence of the occurrence of a balance between electrostatic interactions in both components leading to structures with defined stoichiometry and size. In this context, a temperature increase attempts against the colloid formation as observed in Fig. 4, in which higher crosslinker

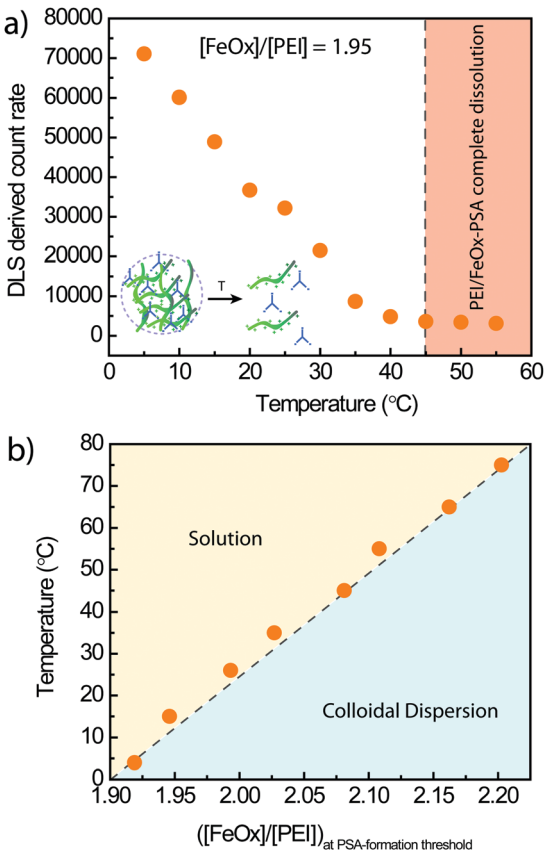

Fig. 4 Temperature response. (a) DLS temperature-trend measurement of a PEI/FeOx-PSA sample with [FeOx]/[PEI] = 1.95 at different temperatures, starting at 5 °C. (b) [FeOx]/[PEI] (mg/ml) ratio at which the transition from a molecular solution to a colloidal dispersion is observed (PSA-formation threshold) at different temperatures.

concentrations are required for inducing colloid formation at higher temperature (Fig. 4b). This situation could be interpreted as the chemical equilibrium between two defined states: molecular solution and aggregates of self-limited size.[28]

For a similar system composed of a mixture of PAH and TPP, Lapitzky *et al.* showed a phase diagram involving different states (molecular solution, colloidal dispersion and adhesive gels) depending on the PAH : TPP ratios.[29] At constant PAH concentration, there is a threshold TPP concentration at which the system collapses into a colloidal dispersion. At this point, the state of minimum energy corresponds to a condensed phase. In the case of the PEI/FeOx system, we observe the same behaviour. In fact, the PEI : FeOx gravimetric ratio was selected to be equal to the colloidal-threshold ratio at 20 °C ([FeOx]/[PEI] = 1.95) when conducting the DLS temperature trend. Then, PEI/FeOx-PSA temperature response could be explained in terms of a variation in the colloidal-threshold ratio with temperature. To test the hypothesis, we measured the colloidal-threshold ratio [FeOx]/[PEI] at different temperatures ranging between 5 and 75 °C and found that this ratio linearly increases with temperature as shown in Fig. 4b.

In summary, we presented a new type of multi-stimuli responsive nanoaggregate using PEI and FeOx as cross-linking agent. The prepared PEI/FeOx-PSAs are responsive to light, reducing agents, and temperature changes. As PSAs can be used as building blocks in surface assemblies,[18,30,31] we believe that the presented PEI/FeOx system not only could be used as solution-phase colloids but also to form multi-stimuli responsive thin films. In PEI/FeOx-PSAs the polyamine only plays a secondary role in the response to stimuli, which is governed by the (photo)(electro)chemistry of the FeOx crosslinker. Thus, analogous PSAs can be obtained by mixing aqueous solutions of FeOx and different polyamines, such as PAH, poly(diallyldimethylammonium chloride), *etc.* A main advantage of the novel multi-stimuli responsive material introduced in this work is its ease of preparation, which involves simple mixing of PEI and FeOx, two inexpensive commercially available reagents. The unique multi-stimuli responsiveness and facile preparation of PEI/FeOx-PSAs make it an attractive candidate for applications and technologies based on smart nanomaterials.

Conflicts of interest

There are no conflicts to declare.

Notes and references

1 H. S. El-Sawy, A. M. Al-Abd, T. A. Ahmed, K. M. El-Say and V. P. Torchilin, *ACS Nano*, 2018, **12**, 10636–10664.
2 S. A. Costa, J. R. Simon, M. Amiram, L. Tang, S. Zauscher, E. M. Brustad, F. J. Isaacs and A. Chilkoti, *Adv. Mater.*, 2018, **30**, 1704878.
3 C. B. Minkenberg, F. Li, P. van Rijn, L. Florusse, J. Boekhoven, M. C. A. Stuart, G. J. M. Koper, R. Eelkema and J. H. van Esch, *Angew. Chem., Int. Ed.*, 2011, **50**, 3421–3424.
4 H. He and B. Xu, *Bull. Chem. Soc. Jpn.*, 2018, **91**, 900–906.
5 R. Cruz-Silva, L. Arizmendi, M. Del-Angel and J. Romero-Garcia, *Langmuir*, 2007, **23**, 8–12.
6 H. Qin, T. Zhang, N. Li, H.-P. Cong and S.-H. Yu, *Nat. Commun.*, 2019, **10**, 2202.
7 Y. Huang, R. Dong, X. Zhu and D. Yan, *Soft Matter*, 2014, **10**, 6121–6138.
8 J. Zhuang, M. R. Gordon, J. Ventura, L. Li and S. Thayumanavan, *Chem. Soc. Rev.*, 2013, **42**, 7421.
9 M. A. C. Stuart, W. T. S. Huck, J. Genzer, M. Müller, C. Ober, M. Stamm, G. B. Sukhorukov, I. Szleifer, V. V. Tsukruk, M. Urban, F. Winnik, S. Zauscher, I. Luzinov and S. Minko, *Nat. Mater.*, 2010, **9**, 101–113.
10 X. Zhang, L. Chen, K. H. Lim, S. Gonuguntla, K. W. Lim, D. Pranantyo, W. P. Yong, W. J. T. Yam, Z. Low, W. J. Teo, H. P. Nien, Q. W. Loh and S. Soh, *Adv. Mater.*, 2019, **31**, 1804540.
11 G. Pasparakis and M. Vamvakaki, *Polym. Chem.*, 2011, **2**, 1234.
12 Y. Yao, J. T. Waters, A. V. Shneidman, J. Cui, X. Wang, N. K. Mandsberg, S. Li, A. C. Balazs and J. Aizenberg, *Proc. Natl. Acad. Sci. U. S. A.*, 2018, **115**, 12950–12955.
13 X. Fu, L. Hosta-Rigau, R. Chandrawati and J. Cui, *Chem*, 2018, **4**, 2084–2107.
14 S. Wang, Q. Zeng, A. Wang, X. Liu, J. Chen, Z. Wang and L. Zhang, *J. Mater. Chem. A*, 2019, **7**, 1069–1075.
15 P. Schattling, F. D. Jochum and P. Theato, *Polym. Chem.*, 2014, **5**, 25–36.
16 F. D. Jochum and P. Theato, *Chem. Soc. Rev.*, 2013, **42**, 7468–7483.
17 Y. Lapitsky, *Curr. Opin. Colloid Interface Sci.*, 2014, **19**, 122–130.
18 S. E. Herrera, M. L. Agazzi, M. L. Cortez, W. A. Marmisollé, C. Bilderling and O. Azzaroni, *Macromol. Chem. Phys.*, 2019, 1900094.
19 J. Yu, D. Javier, M. A. Yaseen, N. Nitin, R. Richards-Kortum, B. Anvari and M. S. Wong, *J. Am. Chem. Soc.*, 2010, **132**, 1929–1938.
20 V. S. Murthy, R. K. Rana and M. S. Wong, *J. Phys. Chem. B*, 2006, **110**, 25619–25627.
21 S. E. Herrera, M. L. Agazzi, M. L. Cortez, W. A. Marmisollé, M. Tagliazucchi and O. Azzaroni, *ChemPhysChem*, 2019, **20**, 1044–1053.
22 H. G. Bagaria and M. S. Wong, *J. Mater. Chem.*, 2011, **21**, 9454–9466.
23 H. Pang, Q. Zhang, H. Wang, D. Cai, Y. Ma, L. Li, K. Li, X. Lu, H. Chen, X. Yang and J. Chen, *Environ. Sci. Technol.*, 2019, **53**, 127–136.
24 S. Goldstein and J. Rabani, *J. Photochem. Photobiol., A*, 2008, **193**, 50–55.
25 I. P. Pozdnyakov, O. V. Kel, V. F. Plyusnin, V. P. Grivin and N. M. Bazhin, *J. Phys. Chem. A*, 2008, **112**, 8316–8322.
26 J. R. Bolton, M. I. Stefan, P.-S. Shaw and K. R. Lykke, *J. Photochem. Photobiol., A*, 2011, **222**, 166–169.
27 J. N. Demas, W. D. Bowman, E. F. Zalewski and R. A. Velapoldi, *J. Phys. Chem.*, 1981, **85**, 2766–2771.
28 E. Piccinini, D. Pallarola, F. Battaglini and O. Azzaroni, *Mol. Syst. Des. Eng.*, 2016, **1**, 155–162.
29 Y. Huang, P. G. Lawrence and Y. Lapitsky, *Langmuir*, 2014, **30**, 7771–7777.
30 W. A. Marmisollé, J. Irigoyen, D. Gregurec, S. Moya and O. Azzaroni, *Adv. Funct. Mater.*, 2015, **25**, 4144–4152.
31 M. L. Agazzi, S. E. Herrera, M. L. Cortez, W. A. Marmisollé, C. von Bilderling, L. I. Pietrasanta and O. Azzaroni, *Soft Matter*, 2019, **15**, 1640–1650.

